RSC Advances

Heterogeneity in GFP expression in isogenic populations of P. putida KT2440 investigated using flow cytometry and bacterial microarrays

Journal:	*RSC Advances*
Manuscript ID	RA-ART-11-2015-023757.R1
Article Type:	Paper
Date Submitted by the Author:	23-Feb-2016
Complete List of Authors:	Arnfinnsdottir, Nina; The Norwegian University of Science and Technology, Physics Bjørkøy, Astrid; The Norwegian University of Science and Technology, NTNU, Department of Physics Lale, Rahmi; The Norwegian University of Science and Technology, Biotechnology Sletmoen, Marit; The Norwegian University of Science and Technology, NTNU, Department of Biotechnology
Subject area & keyword:	Biotechnology - Nanoscience < Nanoscience

Journal Name

ARTICLE

Heterogeneity in GFP expression in isogenic populations of *P. putida* KT2440 investigated using flow cytometry and bacterial microarrays

Received 00th January 20xx,
Accepted 00th January 20xx

DOI: 10.1039/x0xx00000x

www.rsc.org/

N. B. Arnfinnsdottir,[a] A. B. Bjørkøy,[a] R. Lale[b] and M. Sletmoen[b†]

Individual bacteria, even bacteria belonging to an isogenic population under uniform environmental conditions, display phenotypic diversity and variability in gene expression. The increased focus that is lately given to this topic within microbiology and quantitative biology has motivated a quest for new experimental approaches providing insight into phenotypic traits at the single-cell level. In the present paper we investigate the applicability of bacterial microarrays for studies of bacterial populations including their inherent heterogeneity. Results obtained from microscopy of bacterial microarrays are compared to results obtained using flow cytometry. Two different positive-regulated promoter systems were utilized in isogenic cultures of *Pseudomonas putida*, both systems leading to green fluorescent protein production upon induction. Using both experimental approaches, a shift to higher fluorescence intensities with increasing time and increasing inducer concentration was observed, as well as a broadening of the distributions. Additionally, the micrographs of the bacterial microarrays revealed heritable inter-cell variation in green fluorescent protein levels. These observations indicate that for the bacteria studied here the cell to cell heterogeneity in green fluorescent protein expression, as also detected in the flow cytometer, are due to relatively static inter-cell differences.

Introduction

Microbial populations are traditionally studied at the population level, and the parameters determined reflect their average properties. With the development of experimental techniques that enable determination of many of these properties at the single-cell level, the heterogeneity of such populations has been revealed [1, 2]. Today it is therefore well accepted that individual bacteria, even bacteria belonging to an isogenic population under uniform environmental conditions, display phenotypic diversity and variability in their gene expression profile [3-7]. This phenomenon is often referred to as phenotypic heterogeneity, and was recently reviewed [8]. Gaining insight into this heterogeneity is recognized as important for further progress in the understanding of several aspects of the behavior of microbial populations, including stress response, adaptation and robustness towards changing environments [2].

The awareness about the importance of heterogeneity influences the choice of experimental strategies for the study of bacterial populations. When using population-based methods, the phenotypic variability is averaged out [9, 10]. The awareness of this limitation has motivated a quest for new experimental approaches that provide the ability to monitor phenotypic traits at the single-cell level. Phenotypic traits of cells and the distribution of these within a population are generally determined by gene sequencing, mass spectrometry and optical methods such as flow cytometry (FC) or microscopy [11].The combination of single-cell studies with genetically encoded fluorescent proteins that bind to defined structures within or at the surface of the cell has enabled monitoring of cellular properties, beyond size and shape, including protein localization and concentration[12]. In flow cytometers data are obtained on large numbers of cells that are observed one by one as they pass the laser spot of the FC instrument, in a time and labor efficient manner. Furthermore, FCs are widespread and accessible instruments, and FC has therefore been extensively used to gain insight into heterogeneity in biological systems [3, 5, 7] microbial population segregation [13, 14] as well as their response to antibacterial agents[15]. Whilst most flow cytometers have the advantages described above, some instruments have the additional ability to sort cells according to pre-defined phenotypic traits[1, 16, 17]. FC analysis can thus be complemented with further downstream

[a] Biophysics and Medical Technology, Department of Physics, Norwegian University of Science and Technology, NO-7491 Trondheim, Norway.
[b] Department of Biotechnology,Norwegian University of Science and Technology, NO-7491 Trondheim, Norway Address here.
† To whom correspondence should be addressed: Tel: +47 73598694; Fax: +47 73591286; E-mail: marit.sletmoen@ntnu.no.

investigation, such as microscopy, cultivation in liquid or agar plates, or even Omics-based technologies [11, 18-21].

In addition to the many fascinating studies based on FC, significant advances in the understanding of microbial phenotypic heterogeneity have been achieved using single-cell microscopy [22, 23]. The main advantage of this approach compared to FC is its ability to follow individual cells over time, and thus provide insight into the dynamics of cellular behavior. For example, bacterial cell division as well as the production of fluorescent gene-products has been studied at the single-cell level by tracking individual bacteria over prolonged periods of time [4, 22-24]. In some studies, it has been advantageous to separate the cells contained in a cell suspension prior to microscopy studies. Various physical principles have been exploited in microfluidic cultivation devices to trap, isolate and cultivate single-cells [25, 26]. However, 3D trapping and subsequent tracking of individual cells, especially in densely packed microcolonies, is demanding and sophisticated image recognition software is needed. The physical trapping of microorganisms in microfluidic devices can also, due to the closed system required for controlled liquid flow, lead to challenges in later steps aiming at the isolation of cells from the device for further investigations or cultivation.

Bacterial microarrays (BMs), where bacteria are immobilized onto spots on a surface, offer an alternative to the physical trapping in closed chambers in microfluidic devices. When using the microarray approach a high number of cells are studied simultaneously, and statistical information related to the distribution of phenotypic traits within a population can be obtained. Furthermore, microscopy of the BMs provide information on the behavior of the single-cells as a function of time, and the removal of cells from specific spots on the BM, as demonstrated by Iino *et al* who used a micro pipette to collect persister cells, opens for further investigations of cells belonging to interesting sub-populations [27].

We have previously proposed an approach for the preparation of bacterial microarrays (BMs) [28]. These BMs are obtained by immobilizing bacteria onto predefined spots on a glass surface by microcontact printing (μCP) of bioadhesive chemicals [28]. In the current paper we investigate the performance of the BMs for studying variation in phenotypes within isogenic bacterial populations. As part of the study results related to bacterial population heterogeneity obtained using the well-established FC approach are compared with results obtained based on microscopy of BMs. Two different positive-regulated promoter systems were utilized in isogenic cultures of *Pseudomonas putida*, both systems leading to green fluorescent protein (GFP) production upon induction. More precisely, the fluorescence intensity (F_{int}), due to induced GFP production from two positively regulated promoter systems, is quantified at the single-cell level, as a function of time after adding the inducer. The data obtained reveal cell-to-cell heterogeneity in these isogenic populations of bacteria.

Materials and Methods

Pseudononas putida strains and growth conditions

Pseudomonas putida KT2440 (TOL plasmid cured derivative [29]) was grown in Lysogeny Broth (LB) (10g/L tryptone; 5g/L yeast extract; 5g/L NaCl) supplemented with 50 μg/mL kanamycin at 30°C over-night in shake flasks. Two different plasmids were utilized: pSB-B1b and a derivative of pSB-M1g, pHH100-GFP [30]. These plasmids provide the bacteria with the ability to express the GFP variant mut3 from the AraC/P_{BAD} and XylS/P_m positive regulator/promoter systems, respectively. The AraC/P_{BAD} system is induced by arabinose (Sigma-Aldrich), which requires an active uptake by the host cells, whereas the XylS/P_m system is induced by the passively diffusing 3-methylbenzoic acid (MB) (Sigma-Aldrich). Both plasmids are based on a mini-RK2 replicon with a kanamycin gene serving as antibiotic resistance marker. The plasmids were transferred into *P. putida* KT2440 by electroporation [31]. In this paper the cells carrying the plasmid pSB-B1b are referred to as strain A, and the cells carrying the plasmid pHH100-GFP are referred to as strain B.

Analysis of bacterial populations using flow cytometry

Flow cytometry measurements where performed using a Beckman Coulter Gallios (Beckman Coulter). For both strain A and strain B the GFP content of the individual bacteria (F_{int}) was quantified as a function of time after adding the relevant inducer (T_{ind}). Additionally, the inducer was added to four different final inducer concentrations (C_{ind}), studied in separate experimental series. The GFP was excited at 488 nm and the fluorescence detected in the wavelength interval from 505 to 540 nm, in accordance with the emission characteristics of GFP. Measurements were performed every 15 minutes for T_{ind} equal to 3 hours. The samples were prepared for flow cytometry experiments by transferring 6.6 μL of an overnight culture of *P. putida* to vials containing 3 mL LB with varying C_{ind}. For each C_{ind}, three parallel vials were prepared, and small aliquots were extracted and analyzed from each vial at different T_{ind}. Additionally, in each experimental series, a control sample containing bacteria but no inducer was investigated every 30 minutes. When quantifying GFP production in bacteria belonging to strain A the medium contained 1, 10, 25 or 50 mM of the inducer arabinose. When quantifying GFP production in bacteria belonging to strain B the medium contained 0.1, 0.25, 0.5 or 1 mM of the inducer MB. For each series, a total of 20,000 cells were counted. The data were processed using Kaluza (analysis software provided by Beckman Coulter). Based on the three parallel measurements performed for each C_{ind} and at each T_{ind}, the average F_{int} was determined.

Fabrication of bacterial microarrays

BMs of *P. putida* were prepared as previously described [28]. Briefly, the glass bottom (40 mm in diameter) of Willco dishes (WillCo Wells) were PEGylated by immersion in a solution containing 0.1 mg/mL PLL-g-PEG (Susos) for 60 minutes. The pegylated surfaces were then rinsed by immersion in phosphate buffered saline (Sigma Aldrich) followed by MilliQ water before being dryed using nitrogen

gas. A regular pattern of 4 µm in diameter spherical areas of polydopamine (PD) separated by 15 µm was deposited on the PEGylated surface. This was obtained by micro contact printing using a PDMS stamp pre-coated with PD through immersion in a solution containing PD (1 mg/mL in TRIS buffer at pH = 8.5, Sigma Aldrich). Immobilization of *P. putida* on these functionalized glass surfaces was obtained by leaving a drop of overnight culture on the surfaces for 5 minutes. Non-bound bacteria were removed by gentle rinsing with water, and the surfaces containing the arrays were immediately covered with LB.

Microscopy of bacterial microarrays

The BMs of *P. putida* were studied using a Leica SP5 confocal microscope. After positioning the BM on the sample stage of the microscope the LB medium covering the array was replaced with medium containing a predefined concentration of the inducer. The inducer concentrations were identical to those used in the FC experiments. The BMs were imaged every 15 minutes for a duration of three hours using a 20 X air objective (NA =0.7). Both bright field (BF) and fluorescence micrographs were recorded. Fluorescence was detected in the wavelength range 495 to 550 nm. The intensity of the laser (Argon-ion laser line 488 nm) and the detector settings were kept constant throughout the experiments. To compensate for drift of the sample in the z-direction and for potential tilt of the sample holder, causing uneven F_{int} across a micrograph, optical sections were acquired at five different focus positions. The spacing between each section of the z-stack was 500 nm and the center position in the z-stack was the focus determined using the autofocus function in the Leica software LAS AF.

Analysis of micrographs

The maximum intensity z-projection (MIP) function was applied to the z-stack of fluorescence micrographs, using the image processing software ImageJ (www.imagej.net). The corresponding z-stack of BF images was inspected and the image with the highest contrast between background and bacteria was stored, together with the MIP-image, for subsequent image analysis. MATLAB scripts were developed for image processing. In order to minimize effects of field curvature of the objective on the results, only bacteria located inside an inscribed circle of diameter 0.9 x *l* were analyzed, where *l* is the size of the original image (Fig 1A). All cells, including the non-fluorescent ones, were identified. The background of the images was determined by morphological opening on the BF-image using a spherical structuring element of radius 2 pixels. This background was subtracted from the original image one and the intensity and contrast subsequently adjusted (Fig 1B). To reduce noise, a median filter using a 3x3 neighborhood was applied. The resulting image was segmented by the Otsu thresholding method[32]. In order to separate spatially overlapping bacteria, dilated branch points were subtracted from the image. This binary mask (Fig 1C) was then used to localize the pixels of each cell in the fluorescence micrograph. The total fluorescence emitted from a cell was obtained by summarizing the gray values of the pixels of the individual cell.

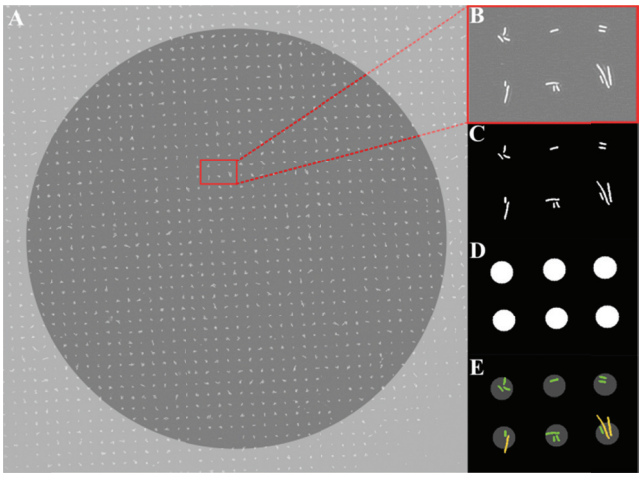

Figure 1: Key steps in the image analysis procedure applied to extract quantitative information from micrographs of BMs. A: Full-sized background-subtracted bright field image of the bacterial microarrays. For illustrative purposes, the image has been subjected to intensity and contrast enhancement. B: A magnified section of the image displayed in A. C: Binary image corresponding to the image section displayed in B. D: Binary image of the spots. E: Image resulting from the merging of image C and D. Bacteria localized inside the PD covered spots are colored green and bacteria localized outside or partly outside these spots are colored yellow.

A binary image containing information about the location of the PD spots (Fig 1D) was created as explained in the following. Since the spots were not visible in neither the BF-image nor the MIP-image, the center coordinates of each spot was approximated based on the fluorescence pattern in the MIP-image, assuming that the bacteria were randomly immobilized onto the PD-spots. Only bacteria localized completely or partly within the spots were included in the subsequent analysis. A radon transform was applied to the fluorescence pattern, to identify the two angles of orientation of the PD-spots. The local fluorescence maxima along the parallel and perpendicular lines at these angles corresponded to the center coordinates of the spots. The interval between the local maxima on each line was approximately 15 µm. With the center coordinates and the radius of each PD-spot determined, the binary image of the microsized pattern could be computed (Fig 1E) and the bacteria classified based on their location relative to a spot.

Results:

Characteristics of the bacterial microarrays

Figure 2 presents representative bright field micrographs obtained for BMs of *P. putida* belonging to strain B. The micrographs were analyzed using a custom-made MATLAB script that allowed extraction of quantitative statistical data. Table 1 presents the results obtained based on micrographs obtained 10 minutes after adding the inducer (T_{ind}=10) for six different BMs. In this analysis a total of 7293 spots were detected, of which 900 were empty (Table 1). The percentage of empty spots varied from 2.1 % to 15.9 %. The average percentage of empty spots was 12.3% and a total of 14,906 bacteria where counted. 10.9% of the detected bacteria were located outside the PD spots while 89.1 % of the bacteria were either inside or partly inside a spot. When excluding the empty spots from the analysis, the average number of bacteria per spot was 2.3.

Table 1: Number and localization of bacteria on PD spots*.

Strain	C_{ind}	Total number of features			Location of bacteria relative to disks		
	mM	Spots	Empty spots	Bacteria	On spots	On borders	Outside
A	50	1250	124	3105	1439	1035	631
	25	1214	189	2397	1740	466	191
	10	1221	102	2431	1805	355	271
	1	1198	145	2521	1705	612	204
B	1	1211	25	2697	2381	356	23
	0.5	1199	315	1755	1121	332	302
SUM		7293	900	14906	10128	3156	1622

**The analysis is based on the first images obtained of the arrays after adding the inducer. These images were obtained at T_{ind} = 5 to 30 minutes.*

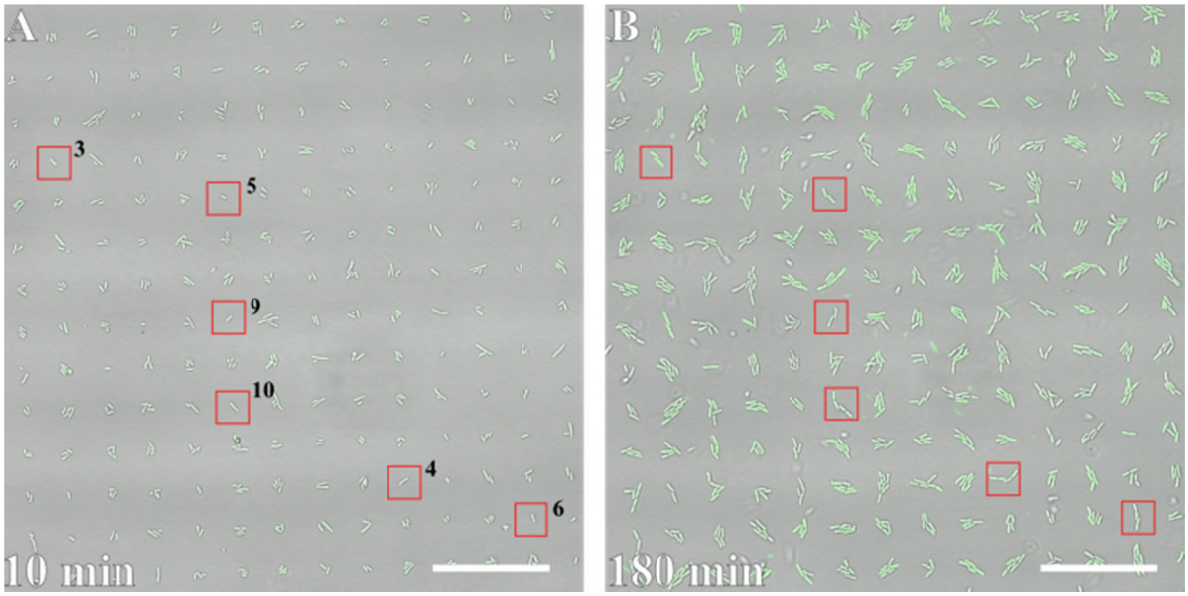

Figure 2: Bright field micrographs of BMs of *P.putida* belonging to strain B. The images were obtained 10 min (A) and 180 min (B) after adding the inducer MB at a concentration C_{ind} equal to 1mM. Scale bar =50 µm. The squares and numbers overlaid on the micrographs identify bacteria that were subjected to the analysis presented in figure 7.

Comparison of results obtained using FC and BMs

F_{int} was determined at the single-cell level as a function of C_{ind} using both FC and the array approach (Fig 3). The points in the graphs reflect the average F_{int} per bacterium determined at different T_{ind}. When using FC this was determined based on an average of three parallel measurements, as described in the materials and methods section. For the BMs the average fluorescence per cell was calculated by summarizing the fluorescence detected for each pixel element contained in the image of the cell. For the bacteria belonging to strain A, the two lowest C_{ind} give rise to only small changes in F_{int} with increasing time after addition of the inducer (Fig 3B). For the two highest C_{ind} investigated, 25 mM and 50 mM, F_{int} increases and reaches a plateau after approximately 100 minutes. This is visible in data obtained both using FC (Fig 3A) and BM (Fig 3B). For the bacteria belonging to strain B, the same tendency is observed: the two lowest C_{ind}, 0.1 mM and 0.5 mM, lead to only small increase in detected fluorescence (Fig 3C). Therefore, for strain B only the two highest concentrations were studied on the BMs (Fig 3D). Whereas the FC data obtained for strain B indicate a plateau in the fluorescence at approximately 160 minutes, this is not visible in the BM data (Fig 3D).

Journal Name

ARTICLE

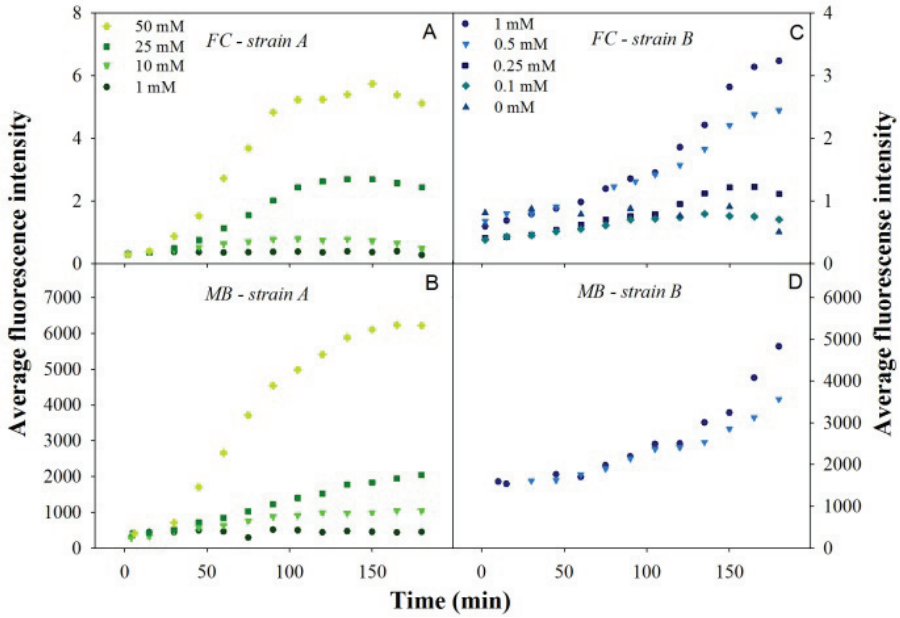

Figure 3: Average fluorescence emitted per bacterium presented as a function of time after adding the inducer. The concentrations displayed in A and C refer to C_{ind} of the inducers arabinose and MB, respectively.

In figure 4 the distribution of average fluorescence intensities are presented for strain A as a function of T_{ind} for three different C_{ind}. The analysis of both FC and BM data reveal a shift to higher fluorescence intensities as well as a broadening of the distribution with increasing T_{ind} and increasing C_{ind}. The average number of cells identified on the BMs underlying the analysis presented in figure 4 were for the examples shown 3084 ± 842 (C_{ind} = 10 mM), 3008 ± 648 (C_{ind} = 25 mM) and 3822 ±975 (C_{ind} = 50 mM). A similar analysis performed for strain B (Fig 5) reveal similar tendencies with respect to increase in average F_{int} and broadening of the intensity distribution. The average number of cells identified on the arrays were 2518 ± 892 (C_{ind} = 0.5 mM) and 3335 ±629 (C_{ind} = 1.0 mM).

Journal Name

ARTICLE

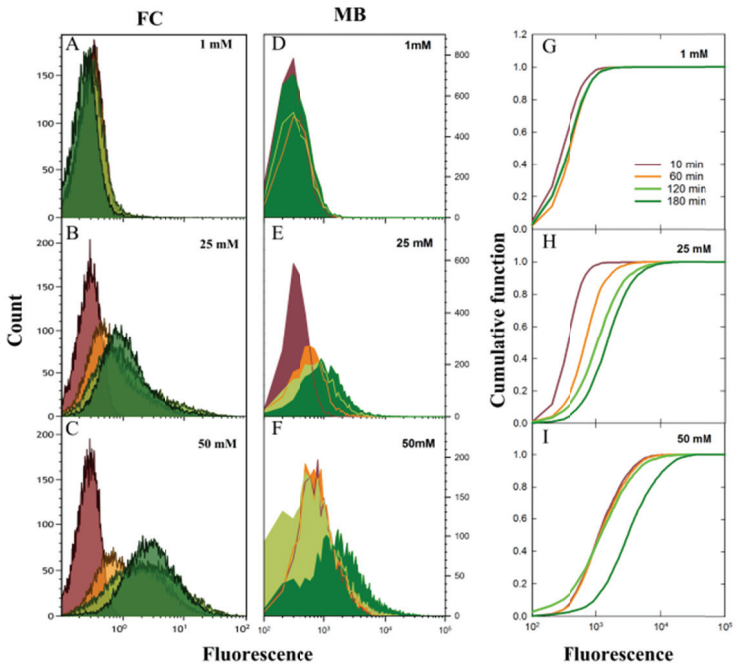

Figure 4: Distributions of F_{int} for bacteria belonging to strain A studied using FC and BMs. A-F: Histograms obtained for strain A based on data obtained using FC (A-C) and BMs (D-F). Data are shown for C_{ind} equal to 1 mM (A and D), 25 mM (B and E) and 50 mM (C and F) and at T_{ind} equal to 5 min (red), 60 min (orange), 120 min (light green), 180 min (dark green). G-I: Cumulative function of the distributions presented in D-F.

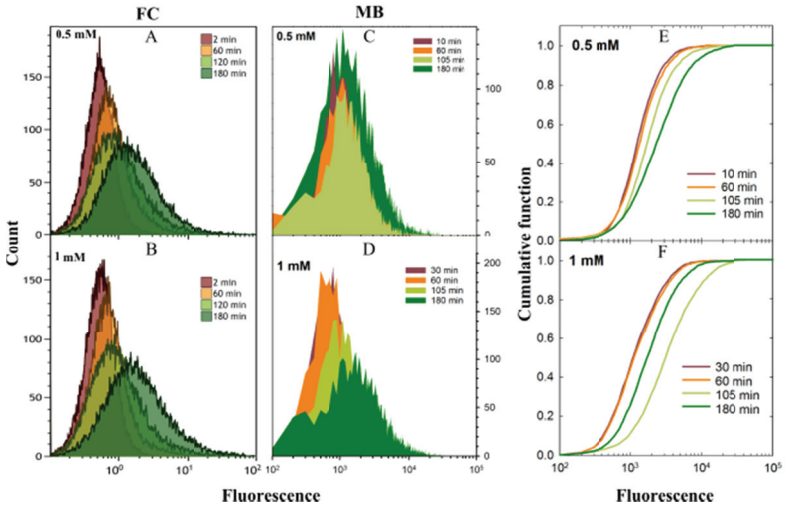

Figure 5: Distributions of F_{int} for bacteria belonging to strain B. A - D: Histograms obtained based on FC (A and B) and BMs (C and D) data. E - F: Cumulative function of the distributions presented in C and D. F_{int} was quantified for C_{ind} equal to 0.5 mM and 1 mM, and at T_{ind} equal to 5 min (red), 60 min (orange), 120 min (light green), 180 min (dark green).

Single-cell fluorescence intensity as a function of T_{ind} and C_{ind}

Microscopy of BMs allowed studying F_{int} for single bacterial cells belonging to strain A or B as a function of T_{int} (Figure 6 and 7). The different rows in figure 6A and 7A show images of single bacteria belonging to strain A or B, respectively, acquired at T_{ind} equal to 15, 60, 120 and 180 minutes. Whereas some bacteria show low and unaltered fluorescence emission upon addition of the inducer (Fig 6B, panel 2), most of the bacteria show increased F_{int} with increasing T_{int} (Fig 6 and 7). However, the rate of the increase in the F_{int}, as well as the final fluorescence level, varies between the different bacteria. Furthermore, the daughter cells seem to inherit the phenological traits of their mother with respect to fluorescence emission (Fig 6B and 7B).

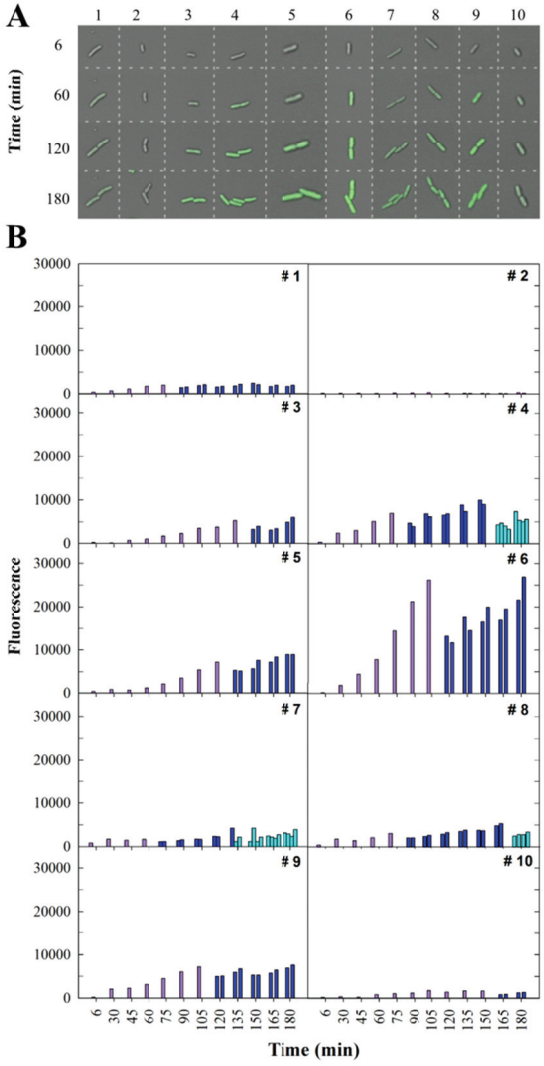

Figure 6: Increase in fluorescence emitted from bacteria belonging to strain A as a function of T_{ind} (C_{ind} = 50 mM). A: Magnified sections of fluorescence micrographs displaying 10 different bacteria and their daughter cells. The same cells are identified in micrographs acquired at T_{ind} equal to 15, 60, 120 and 180 minutes. B: Average F_{int} determined for the cells displayed in A as a function of increasing T_{ind}. F_{int} for the first, second and third generation of bacteria is shown in violet, blue and turquoise, respectively.

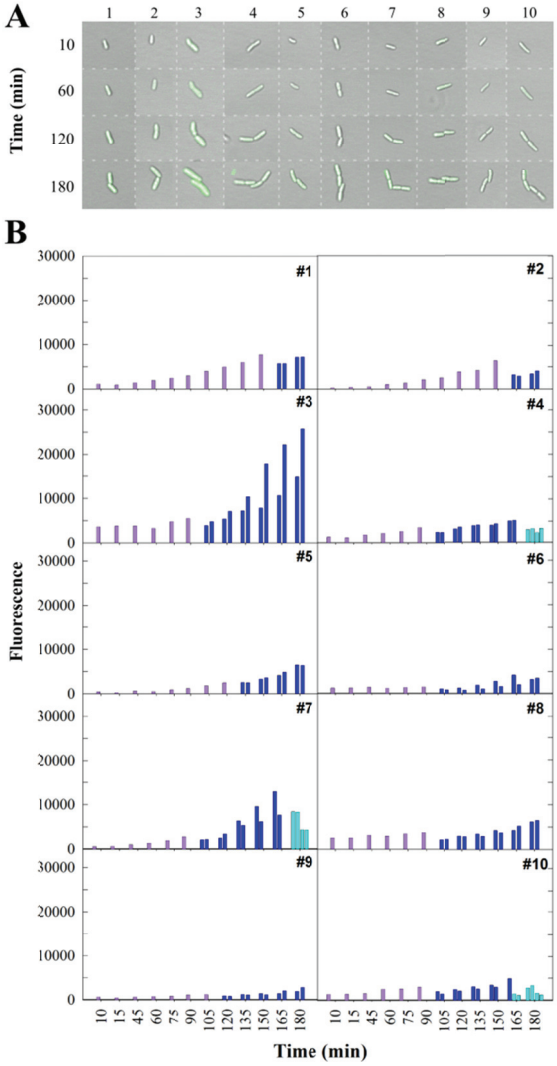

Figure 7: Increase in fluorescence emitted from bacteria belonging to strain B as a function of increasing T_{ind} (C_{ind} =1 mM). A: Magnified sections of fluorescence micrographs displaying 10 different bacteria and their daughter cells. The same cells are identified in micrographs acquired at T_{ind} equal to 15, 60, 120 and 180 minutes. B: Average F_{int} determined for the cells displayed in A as a function of increasing T_{ind}. F_{int} for the first, second and third generation of bacteria is shown in violet, blue and turquoise, respectively.

Journal Name

ARTICLE

Upon cell division the size of the bacterium, and thus the total intensity of the emitted fluorescence, is reduced by approximately 50%, whereas the average fluorescence intensity per pixel element remains unchanged (Figure 8). Some of the bacteria studied divided twice during the three hours' time period they were studied (Fig 6 panel 4, 7 and 8, figure 7 panel 4 and 7). These observations indicate a generation time in the interval 75 to 90 minutes. The location of the bacteria presented in figure 6 with respect to the cumulative distributions of the bacteria (figure 4) reveal that the bacteria remain close to a defined percentile in the distributions (Figure 9).

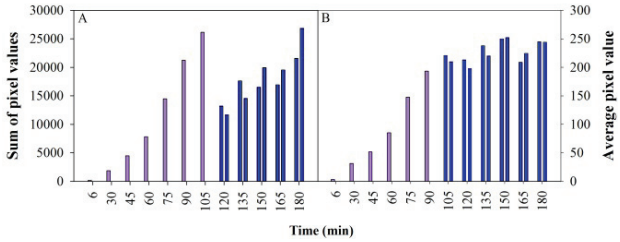

Figure 8: Increase in fluorescence intensity for a single bacterium as a function of increasing T_{ind}. A: F_{int} defined as the sum of the fluorescence determined in each of the pixel elements in the image of the bacterium. B: Fluorescence defined as the average value of the pixels elements in the image of the bacterium. The analysis is performed on the bacterium displayed in figure 6A #6.

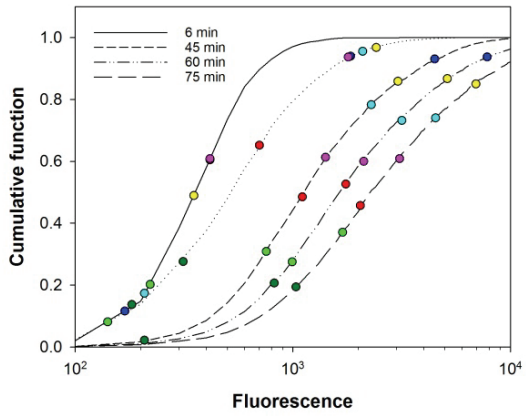

Figure 9: Cumulative function presenting the increase in F_{int} with increasing T_{ind}. The lines reflect the average F_{int} of a population of *P.putida* belonging to strain A. The symbols represent the fluorescence determined for some of the individual bacterial cells presented in figure 6. Among the cells presented in figure 6, the ones that divided prior to T_{ind} = 60 min or that showed very low and non-increasing F_{int} are not included.

Discussion

We have proposed an approach that makes imaging of high numbers of well separated single-cells possible in a non-labor-intensive way. The approach combines an advantage of FC, its ability to study high numbers of individual cells, with the advantages of fluorescence microscopy with respect to resolution and ability for time-lapse studies. The proposed method for the preparation of BMs gave arrays characterized by high regularity at short waiting times after immobilizing the bacteria (Fig 2 and table 1). The observed ability of the bacteria to divide on the arrays (Fig 2 right image) reflects the viability of the immobilized bacteria and is consistent with the reported results of a live/dead assay [28].

Fluorescence microscopy images often contain a vast amount of information, which is often hidden behind various sources of noise, convoluted with other information and stochastic in nature. Accessing the desired biological information can thus in many cases be facilitated by computational image analysis. The image analysis described in the current paper (Fig 1) illustrates how extraction of quantitative statistical data can be efficiently performed, and the BMs allow such analysis to be performed on a high number of cells. The automated analysis of high resolution micrographs of BMs is therefore a useful approach in studies aiming at revealing heterogeneity in bacterial behavior.

In order to validate the proposed approach, data obtained from the quantitative analysis of the BMs were compared to data obtained using FC (Fig 3). Similar increase in average F_{int} was observed using both approaches. The similarity of the data obtained using the two methods illustrate that the array approach provides correct information concerning the average behavior displayed by the populations. Good correspondence between the information obtained by the two techniques is also observed related to the distribution of average fluorescence intensities as determined on the single-cell level (Fig 4 and 5). Using both approaches, a shift to higher fluorescence intensities with increasing time and increasing C_{int} was observed, as well as a broadening of the distributions.

The fluorescence micrographs obtained for the BMs revealed that average F_{int} per cell as a function of T_{ind} vary significantly between the different bacteria. (Fig 6 and 7) For some of the bacteria F_{int} increased from 170 to 26140, a 15,000 % increase with time after addition of the inducer (Fig 6 #6). For other bacteria no increase in F_{int} was observed upon addition of the inducer (Fig 6 #2), and the remaining bacteria showed an increase in F_{int} intermittent of these

two extremes. The variation in F_{int} over time detected for a given bacterium was relatively small compared to the variation observed between the different bacteria (Fig 6 and 7). A significant fraction of the bacteria underwent cell division while being immobilized on the array. Cell division of bacteria immobilized to surfaces was also previously observed using AFM[33]. The fluorescence images reveal that the daughter cells show similar behavior as the mother cells with respect to F_{int} (Fig 6 and 7). F_{int}, reflecting the GFP concentration within the bacterium, thus appears to be a property that is inherited by the daughter cells. F_{int} deduced from the growth of the individual bacteria indicate that they follow the same percentile within the distribution (Fig 9). These observations indicate that for the bacteria studied here the cell to cell heterogeneity in GFP production, as also detected in the flow cytometer, are due to relatively static inter-cell differences.

Stochasticity in bacterial populations is known to result either from intrinsic or extrinsic sources. Intrinsic noise can be the result of stochastic promoter activation, promoter deactivation, and the rate of production and decay of mRNA and proteins, whereas extrinsic noise refers to the variation observed from external sources to the biochemical process and gene expression [4, 34]. In this study we have utilized two different positive regulated promoter systems, on the same replicon, which led to the observation of distinct heritable inter-cell variation in GFP levels in *P. putida* KT2440. What unifies both systems is the use of same replicon, the reporter gene, and the bacterial strain. The plasmid replicon utilized, mini-RK2 is a low-copy number plasmid with 5 to 8 copies per chromosome The mini-RK2 plasmid originates from the RK2 plasmid (60kb), but lacks the partitioning system which for intact RK2 leads to a plasmid localization inside the nucleoid in mid- or quarter-cell positions[35], ensuring the daughter cells receiving at least one copy of the plasmid The lack of this system leads to, in *E. coli*, localization of the mini-RK2 plasmid at the cell poles outside of the nucleoid as clusters [35] hence cell-to-cell variation in plasmid copy numbers. The localization characteristics of mini-RK2 replicon in *P. putida* are currently not known. However, if also this plasmid clusters at the cell poles during cell division this might account for the observed cell-to-cell variation (Fig 6 and 7).

The biochemical steps involved in production of GFP, as well as cell-to-cell variation in inducer uptake might be influenced by cell-specific factors which may also contribute to the observations described in figure 6 and 7. Regardless of the molecular explanation the variation in the observed phenotypic trait is a heritable one as the daughter cells formed exhibits the same level of GFP expression as the mother cell.

Conclusion

In this work, the applicability of bacterial microarrays for studies of heterogeneity in isogenic cultures of *Pseudomonas putida* was studied. A comparison of results obtained from microscopy of BMs with results obtained using FC allowed validating the BM approach. Using both experimental approaches, a shift to higher fluorescence intensities with increasing time and increasing inducer concentration was observed, as well as a broadening of the distributions. The two different promoter systems studied both led to the observation of distinct heritable inter-cell variation in GFP levels in *P. putida* KT2440. These observations indicate that for the bacteria studied here the cell to cell heterogeneity in GFP expression, as also detected in the flow cytometer, are due to relatively static inter-cell differences.

Acknowledgments

The Research Council of Norway is acknowledged for the support to the Norwegian Microand Nano-Fabrication Facility, NorFab (197411/V30).

References

1. S. Müller and G. Nebe-von-Caron, *FEMS Microbiology Reviews*, 2010, **34**, 554-587.
2. C. Dusny, A. Grunberger, C. Probst, W. Wiechert, D. Kohlheyer and A. Schmid, *Lab Chip*, 2015, **15**, 1822-1834.
3. E. M. Ozbudak, M. Thattai, I. Kurtser, A. D. Grossman and A. van Oudenaarden, *Nat Genet*, 2002, **31**, 69-73.
4. M. B. Elowitz, A. J. Levine, E. D. Siggia and P. S. Swain, *Science*, 2002, **297**, 1183-1186.
5. W. J. Blake, M. Kaern, C. R. Cantor and J. J. Collins, *Nature*, 2003, **422**, 633-637.
6. I. Golding, J. Paulsson, S. M. Zawilski and E. C. Cox, *Cell*, 2005, **123**, 1025-1036.
7. J. R. S. Newman, S. Ghaemmaghami, J. Ihmels, D. K. Breslow, M. Noble, J. L. DeRisi and J. S. Weissman, *Nature*, 2006, **441**, 840-846.
8. M. Ackermann, *Nat Rev Micro*, 2015, **13**, 497-508.
9. J. E. Ferrell and E. M. Machleder, *Science*, 1998, **280**, 895-898.
10. J. M. Skotheim, S. Di Talia, E. D. Siggia and F. R. Cross, *Nature*, 2008, **454**, 291-296.
11. M. Jahn, J. Seifert, M. von Bergen, A. Schmid, B. Buhler and S. Muller, *Curr Opin Biotech*, 2013, **24**, 79-87.
12. D. M. Chudakov, M. V. Matz, S. Lukyanov and K. A. Lukyanov, *Physiol Rev*, 2010, **90**, 1103-1163.
13. A. Patkar, N. Vijayasankaran, D. W. Urry and F. Srienc, *Journal of Biotechnology*, 2002, **93**, 217-229.
14. N. R. Abu-Absi, A. Zamamiri, J. Kacmar, S. J. Balogh and F. Srienc, *Cytometry Part A*, 2003, **51A**, 87-96.
15. W. Liu, M. H. Cai, Y. G. He, S. Wang, J. W. Zheng and X. P. Xu, *Rsc Adv*, 2015, **5**, 84432-84438.
16. N. G. Howlett and S. V. Avery, *FEMS Microbiology Letters*, 1999, **176**, 379-386.
17. D. Mattanovich and N. Borth, *Microbial Cell Factories*, 2006, **5**, 12-12.
18. T. Bernas, G. Grégori, E. K. Asem and J. P. Robinson, *Molecular & Cellular Proteomics*, 2006, **5**, 2-13.
19. C. Wiacek, S. Müller and D. Benndorf, *PROTEOMICS*, 2006, **6**, 5983-5994.

20. N. Jehmlich, T. Hübschmann, M. Gesell Salazar, U. Völker, D. Benndorf, S. Müller, M. von Bergen and F. Schmidt, *Appl Microbiol Biotechnol*, 2010, **88**, 575-584.
21. M. Jahn, C. Vorpahl, D. Turkowsky, M. Lindmeyer, B. Buhler, H. Harms and S. Muller, *Anal Chem*, 2014, **86**, 5969-5976.
22. J. W. Young, J. C. W. Locke, A. Altinok, N. Rosenfeld, T. Bacarian, P. S. Swain, E. Mjolsness and M. B. Elowitz, *Nat Protoc*, 2012, **7**, 80-88.
23. K. M. Münch, J. Müller, S. Wienecke, S. Bergmann, S. Heyber, R. Biedendieck, R. Münch and D. Jahn, *Applied and Environmental Microbiology*, 2015, **81**, 5976-5986.
24. E. Verplaetse, L. Slamti, M. Gohar and D. Lereclus, *Mbio*, 2015, **6**.
25. J. Nilsson, M. Evander, B. Hammarstrom and T. Laurell, *Anal Chim Acta*, 2009, **649**, 141-157.
26. A. Grunberger, W. Wiechert and D. Kohlheyer, *Curr Opin Biotech*, 2014, **29**, 15-23.
27. R. Iino, Y. Matsumoto, K. Nishino, A. Yamaguchi and H. Noji, *Frontiers in Microbiology*, 2013, **4**, 300.
28. N. B. Arnfinnsdottir, V. Ottesen, R. Lale and M. Sletmoen, *Plos One*, 2015, **10**.
29. M. I. Ramos-González, M. J. Campos and J. L. Ramos, *Journal of Bacteriology*, 2005, **187**, 4033-4041.
30. S. Balzer, V. Kucharova, J. Megerle, R. Lale, T. Brautaset and S. Valla, *Microbial Cell Factories*, 2013, **12**, 26-26.
31. K.-H. Choi, A. Kumar and H. P. Schweizer, *Journal of Microbiological Methods*, 2006, **64**, 391-397.
32. N. Otsu, *Systems, Man and Cybernetics, IEEE Transactions on*, 1979, **9**, 62-66.
33. T. J. Gunther, M. Suhr, J. Raff and K. Pollmann, *Rsc Adv*, 2014, **4**, 51156-51164.
34. M. Kaern, T. C. Elston, W. J. Blake and J. J. Collins, *Nat Rev Genet*, 2005, **6**, 451-464.
35. C. Verheust and D. R. Helinski, *Plasmid*, 2007, **58**, 195-204.

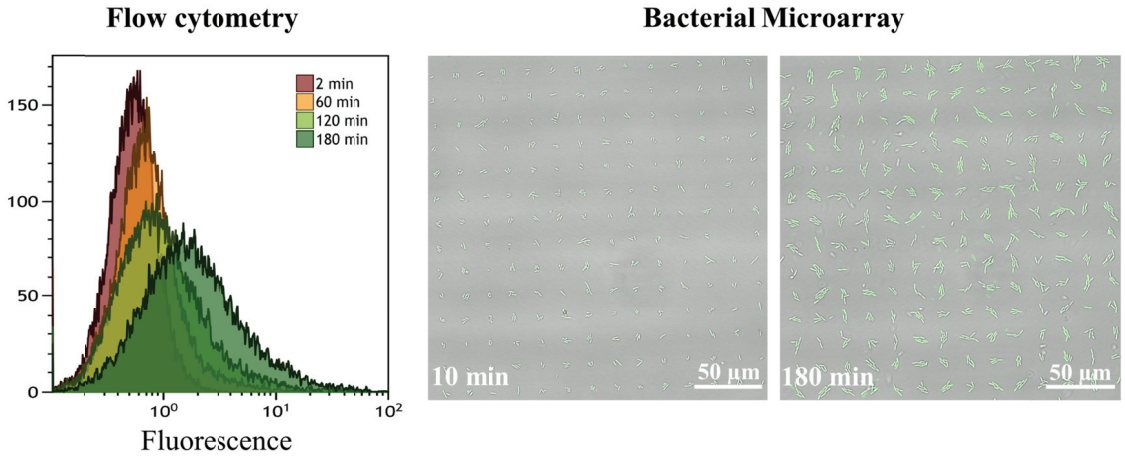

Distributions of fluorescence intensities were determined using both flow cytometry and bacterial microarrays for populations of *Pseudomonas putida* expressing GFP upon addition of an inducer. The data reveal increasing fluorescence intensities, and also a broadening of the population distributions, with increasing time after introducing the inducer. A quantitative analysis of the micrographs indicated that the observed distributions in fluorescence intensities are due to relatively static inter-cell differences.